physica status solidi a
www.pss-a.com

# Growth and Characteristics of C8-BTBT Layer on C-Sapphire Substrate by Thermal Evaporation

*Aye M. Moh,* Pei Loon Khoo, Kimihiro Sasaki, Seiji Watase, Tsutomu Shinagawa, and Masanobu Izaki*

**The organic semiconductor 2,7-dioctyl[1]benzothieno[3,2-b][1]benzothiophene (C8-BTBT) is deposited on a single crystal (0001) $Al_2O_3$ (C-sapphire) by a vacuum thermal evaporation, and effects of the layer thickness and preparation temperature on structural, morphological, optical, and electrical characteristics are investigated with X-ray diffraction, atomic force microscopy observation, optical absorption measurement, and resistivity measurement with and without light irradiation. The C8-BTBT layers possess the (001) out-of-plane orientation irrespective of the layer thickness and preparation temperature. The C8-BTBT grains are growing up in direction parallel to the substrate surface keeping almost constant height, and the continuous layer is formed by the coalescence of the C8-BTBT grains. The grain size of the continuous C8-BTBT layer increases with raise in preparation temperature. The optical band gap energy could be estimated to be 3.32–3.35 eV regardless of the layer thickness and preparation temperature. The electrical resistivity decreases from $2.1 \times 10^6$ to $1.2 \times 10^2\ \Omega$ cm with increase in the preparation temperature due to the increase in the grain size, and the light irradiation induce the drastical decrease to 42–28 Ω cm.**

## 1. Introduction

The π-conjugated organic semiconductors have been technologically great impact in fields of organic electronics; organic thin layer transistors (OTFT), organic field effect transistors (OFETs), organic light-emitting diodes (OLEDs), and organic photovoltaics (OPVs).[1–4] The electrical characteristics including the charge transportation property[5,6] strongly affects the performance of electronic devices and relates to the structure, molecular orientation, morphology,[7] grain size, and defect density of organic semiconductor layers.[8,9] The surface defects such as steps and vacancies of the underlying substrate could influence the structure of the molecular ordering and subsequent growth of the organic layers.

Molecular semiconductor of π-conjugated core with two octyl chains, 2,7-dioctyl[1] benzothieno[3,2-b][1] benzothiophenes (C8-BTBT) is one of the promising semiconducting materials for fabricating the organic electronic devices because of their high mobility value of 31.3 and 43 $cm^2 V^{-1}s^{-1}$.[10,11] The C8-BTBT layer has been prepared by several techniques of organic molecular beam evaporation, inkjet printing, and spin-coating method, and the mobility value changed depending on the preparation techniques.[9,11–12] Furthermore, the orientation of C8-BTBT molecules changed depending on the substrate materials of graphene, boron nitride, and $SiO_2$/Si.[11,13–14] However, the growth of C8-BTBT molecules on single crystal sapphire substrate appropriate to consider the structural relation between the organic layers and single crystal substrate have not been reported yet. The C8-BTBT layer growth still remains rich subject to be better understanding of the linkage between the structural properties and electrical properties of C8-BTBT active layer.

In this study, we prepared (001)-orientated C8-BTBT layers on a single crystal $Al_2O_3$ (C-sapphire) substrate by a vacuum thermal evaporation. The structural, optical, and electrical properties were investigated with X-ray diffraction (XRD), atomic force microscopy (AFM), optical absorption spectra measurement, and van-der-Pauw method to make the growth process clear and examine the effects of the layer thickness and preparation temperature on the electrical characteristics.

## 2. Experimental Section

Organic semiconductor layers of 2,7 dioctyl[1] benzothieno-[3,2-b][1]benzothiophene(C8-BTBT) were prepared on a (0001) [11$\underline{2}$0] $Al_2O_3$ single crystal (C-sapphire) substrates at thickness ranging from 5 to 100 nm and preparation temperatures of 300, 343, and 373 K by a vacuum thermal evaporation. The C8-BTBT powder (99% purity, Sigma–Aldrich) was used as a source material in the vacuum evaporation system (ULVAC, VTS-350ERH/M) connected with turbo molecular pump and oil-free scroll vacuum pump. The one side polished C-sapphire substrates

A. M. Moh, P. L. Khoo, K. Sasaki, Dr. M. Izaki
Toyohashi University of Technology
Toyohashi, Aichi 441-8580, Japan
E-mail: aye@tf.me.tut.ac.jp
Dr. S. Watase, Dr. T Shinagawa
Morinomiya Center
Osaka Research Institute of Industrial Science and Technology (ORIST)
Osaka 536-8553, Japan
The ORCID identification number(s) for the author(s) of this article can be found under https://doi.org/10.1002/pssa.201700862.

DOI: 10.1002/pssa.201700862

 

were annealed in air at 1200 °C for 1 hr. The preparation was carried out in the pressure around $4 \times 10^{-5}$ Pa, and C8-BTBT layers were deposited in the thickness ranging from 5 to 100 nm at a constant deposition rate 0.1 nm/s and preparation temperatures 300, 343, and 373 K. The deposition rate was monitored by a quartz crystal oscillator sensor in a vacuum evaporation system (ULVAC, CRTM-6000G). The thickness of the C8-BTBT layers were determined by using a surface profiler measurement system (ULVAC, DekTak150).

Conventional out-of-plane X-ray diffraction were performed by a θ/2θ scanning technique using Rigaku RINT 2500 X-ray diffractometer at monochromatic CuKα radiation operated at 20 kV, 10 mA with a wavelength (λ = 0.154059 nm). X-ray diffraction spot patterns were recorded by using 2D imaging plate detector with monochromatic Cu $K_\alpha$ radiation using Rigaku RINT-Rapid II. Surface morphologies were observed by an atomic force microscopy (AFM, Shimadzu, SPM-9700 Kai) in non-contact mode in air. Absorption spectra measurements were performed using a UV-VIS-NIR spectrophotometer (HITACHI, U4100) with a reference of (0001) C-sapphire bare substrate. Electrical properties were measured by using van-der-Pauw method at room temperature (Toyo Technica, Resitest 8310) with and without AM1.5G light irradiation (Asahi Spectra, HALC100).

## 3. Results and Discussion

**Figure 1** shows out-of-plane X-ray diffraction patterns for 5, 10, 15, 50, and 100-nm-thick C8-BTBT layers prepared on C-sapphire substrate at 300 K, for 100 nm-thick layers prepared at 300, 343, and 373 K, and the dependence of the FWHM values on the thickness. Two peaks were observed at around 6.1 and 9.1° on X-ray diffraction patterns irrespective of the layer thickness and preparation temperature. These two peaks could be identified as (002) and (003) planes of the C8-BTBT layer with the characteristic monoclinic lattice. The (001) out-of-plane orientation was developed irrespective of the preparation temperature. The peak intensity increased with increase in layer thickness keeping almost constant intensity ratio. The peak angle of (002) peak showed almost constant value of 6.1 degree regardless of the layer thickness and preparation temperature. The FWHM value drastically decreased from 0.3–0.6 degree to 0.1° with increase in layer thickness from 5 nm to 50 nm and then showed almost constant value. The FWHM value relates to the grain size and heterogeneous strain, and the decrease in FWHM value gives increase in the grain size and/or decrease in the heterogeneous strain.

**Figure 2** shows the X-ray diffraction patterns recorded by the imaging plate for annealed bare C-sapphire substrate with the radial and circumferential directions represent by the 2θ and β angles and 100-nm-thick C8-BTBT layers deposited at 300 and 343 K. Many diffraction spots could be observed on the XRD image for 100 nm-C8-BTBT layers in addition to the spots observed for bare C-sapphire substrate. Similar spot pattern represented by arrow ① and ② could be observed irrespective of the layer thickness and preparation temperature, and two diffraction spots represented by arrow ① were identified as (002)

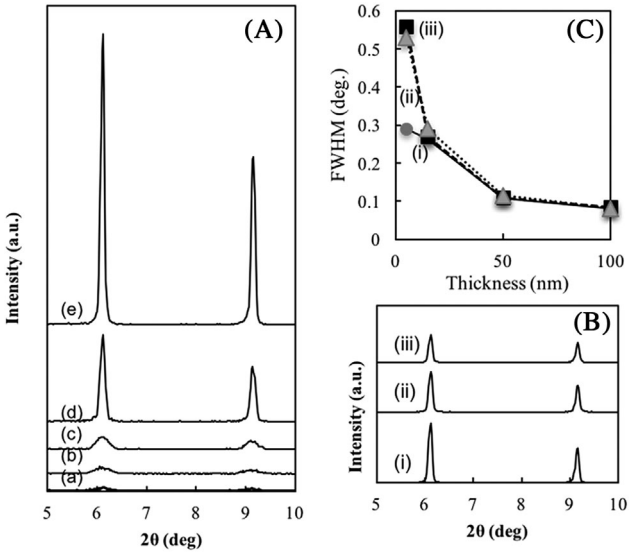


**Figure 1.** X-ray diffraction patterns (A) of 5 (a), 10 (b), 15 (c), 50 (d), 100-nm thick-C8-BTBT layers (e) prepared on C-sapphire substrate at 300 K and (B) 100-nm-thick layers prepared at 300 (i), 343 (ii), and 373 K (iii), and the dependence of the FWHM values on the thickness (C).

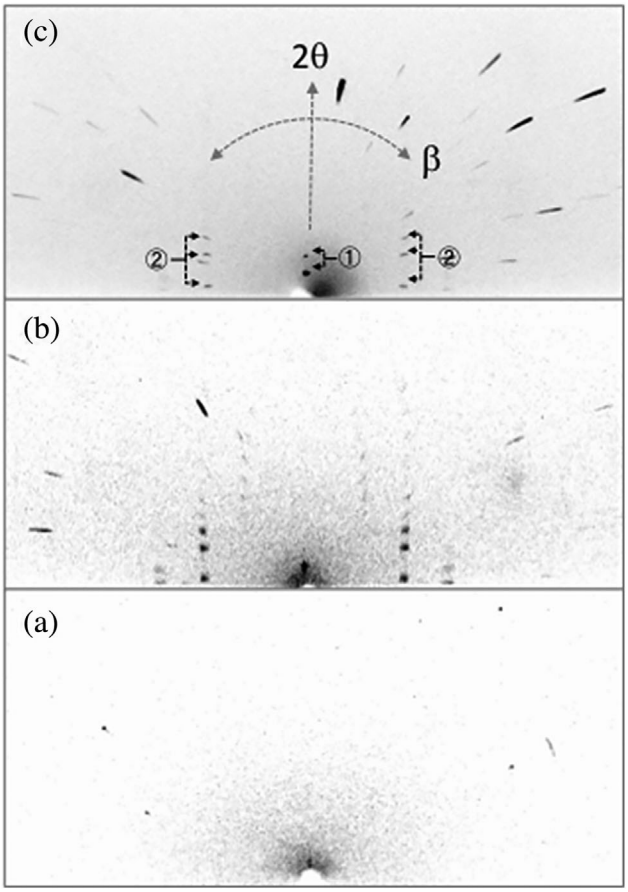


**Figure 2.** X-ray diffraction patterns recorded for bare C-sapphire substrate (a), and 100-nm-thick C8-BTBT layers deposited on C-sapphire substrate at 300 K (b), and 343 K (c) with imaging plate.

and (003) planes of C8-BTBT layer. Debye ring could not be observed on the XRD image irrespective of the layer thickness and preparation temperature. The out-of-plane XRD represented in Figure 1 showed the formation of the (001) out-of-plane preferred orientation, and the similar spot patterns suggested that the preferred orientation including the in-plane orientation was almost the same, although it was difficult to estimate quantitatively.

The C8-BTBT possessed the monoclinic lattice with lattice constants of 0.5927 nm in *a*-axis, 0.788 nm in *b*-axis, 2.918 nm in *c*-axis, and 92.443° in β-angle, [15] and $Al_2O_3$ possessed the characteristic hexagonal lattice with lattice constants of 0.47589 nm in *a*-axis, and 1.2991 nm in *c*-axis.[16] The lattice mismatch was estimated to be −24.5% along *a*-axis, and +4% along *b*-axis for the lattice relationship of (001)[100]C8-BTBT//(0001)[11$\underline{2}$0]$Al_2O_3$. The (001)-out-of-plane orientation was developed for the C8-BTBT layer on C-sapphire substrate, inspite of the large lattice mismatch.

The spot pattern suggested that the C8-BTBT layers possessed an in-plane orientation in addition to the (001)-out-of-plane orientation and a lattice relationship to the C-sapphire substrate, in spite of the large lattice mismatch. It was difficult to decide the in-plane lattice relationship with X-ray diffraction techniques used in this study due to the characteristic monoclinic lattice of the C8-BTBT and difficulty in the precise analysis, resulting in not being able to identify whether the C8-BTBT layer was a single crystal or polycrystalline with the (001)-out-of-plane orientation and not identified in-plane orientation.

**Figure 3** shows AFM images for the bare C-sapphire substrate and C8-BTBT layers prepared at 300 K with the thickness of 5, 10, 15, 50, and 100 nm. Several atomic steps, approximately 1 μm in interval could be observed on the AFM image, although the image was with noise. Isolated C8-BTBT islands were formed on the C-sapphire substrate, and the height of 11.5–11.8 nm corresponded to be approximately fourth the *c*-axis values of C8-BTBT molecule. The islands were growing up in direction parallel to the substrates surface, keeping the almost constant height with the smooth top surface, resulting in the formation of continuous layer, although some pores could be located between the grains. The surface roughness Ra was estimated to be 1.26 nm at 10-nm-thick C8-BTBT layer. According to the AFM observation of 15-nm-thick C8-BTBT layer, the small grains with the size of 0.2–0.68 μm stacked on the continuous layer, although the Ra was estimated to be 1.23 nm almost same as that at 10-nm-thick layer. The small grains were growing up to 0.3–1 μm with keeping smooth top surface and terraces as represented in inset could be observed clearly, indicating that the small grains grew by layer-by-layer growth. The surface roughness increased from 1.23 nm at 15-nm-thickness to 5.2 nm at 100-nm-thickness via 3.1 nm at 50-nm-thickness, suggesting that the small grains grew up in direction normal to the substrate surface. The C8-BTBT layer grew up on the C-sapphire substrates by following process. The (001)-orientated C8-BTBT islands were growing up in direction parallel to the substrate surface until forming the continuous layer by the coalescence, and then small grains grew on the continuous layers by layer-by-layer growth.

The growth of the C8-BTBT layer at 343 and 373 K proceeded by the similar process as that at 300 K. AFM images for C8-BTBT layers prepared at 343 K with the thickness of 5, 10, 15, 50, and 100 nm which were shown in **Figure 4**. The height of the C8-BTBT islands before the coalescence changed depending on the preparation temperature, and the height at 343 K was estimated to be 2.4–2.9 nm nearly corresponding to the c-axis values of C8-BTBT lattice. The size of grain grown on the continuous layer after the coallescence increased from 0.45–0.76 to 1.8–2.7 μm with increase in thickness from 15 to 100 nm.

The C8-BTBT islands prepared at 373 K showed approximately 0.69 μm in size at average thickness of 5 nm and increased to approximately 4.0 μm at the 100-nm-thickness after the coalescence of islands. The change in the surface roughness was similar tendency to that at 343 K, and the Ra value was estimated to be 9.2 nm at 100-nm-thickness.

**Figure 5** shows the dependence of the surface roughness on the C8-BTBT layer thickness at 300 and 343 K and the effects of the preparation temperature on the C8-BTBT grain size at the thickness of 5 and 100 nm. The surface roughness, Ra showed almost constant value up to 15 nm irrespective of the preparation temperature, because C8-BTBT islands with smooth top surface grew in direction parallel to the substrate surface. And, then the Ra value increased with increase in the layer thickness, as the

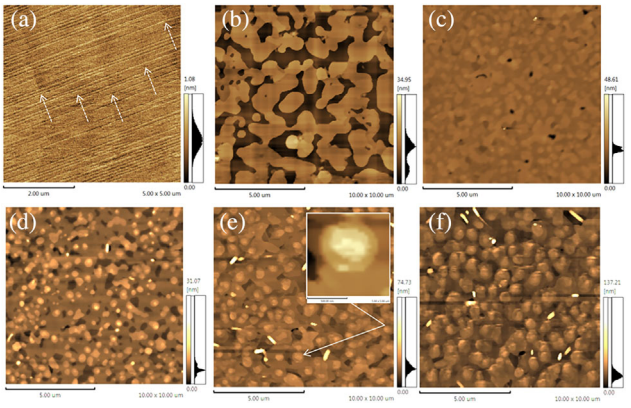


**Figure 3.** AFM images for bare C-sapphire substrate (a) and C8-BTBT layers prepared at 300 K with the thickness of 5 (b), 10 (c), 15 (d), 50 (e), and 100 nm (f).

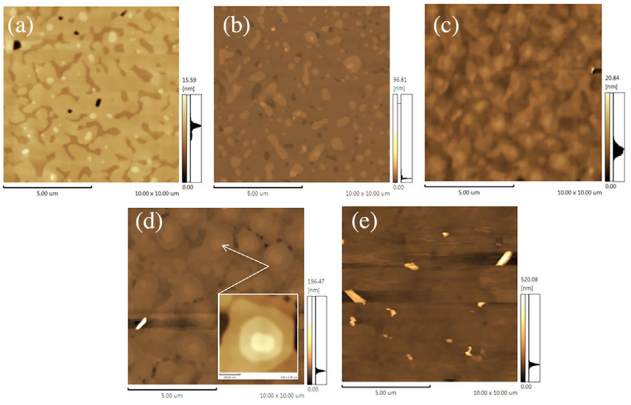


**Figure 4.** AFM images for C8-BTBT layers prepared at 343 K with the thickness of 5 (a), 10 (b), 15 (c), 50 (d), and 100 nm (e).

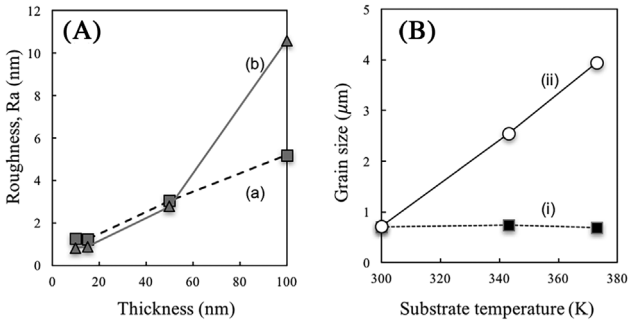


**Figure 5.** Dependence (A) of the surface roughness (Ra) on the C8-BTBT thickness at 300 (a) and 343 K (b), and the Effect (B) of the substrate temperature on the C8-BTBT grain size at the average thickness of 5 (i) and 100 nm (ii).

growth of the C8-BTBT transferred to layer-by-layer growth after forming continuous layer.

The grain size of C8-BTBT islands at the 5-nm-thickness showed almost constant value of 0.69–0.74 μm irrespective of the preparation temperature, indicating that the preparation temperature did not affect the size of C8-BTBT islands directly deposited on C-sapphire substrate. The clear effect of the preparation temperature on the grain size of C8-BTBT layer was observed at the layer thickness of 100 nm. These results suggested that the growth of C8-BTBT islands before the coalescence of the C8-BTBT layer was dominated by the substrate material and the growth after forming the continuous layer was affected by the preparation temperature.

**Figure 6** shows absorption spectra for 5, 10, 15, 50, and 100 nm-thick-C8-BTBT layers deposited on C-sapphire substrate at preparation temperature at 300 K. The absorption spectra were almost the same in profile and peak wavelength irrespective of the thickness and the absorbance increased with increase in layer thickness. A weak shoulder was observed at the wavelength of approximately 340 nm, and maximum absorption peaks were seen at the wavelength of 358 nm for all C8-BTBT layers. The spectra were almost the same in profile and peak wavelength as that already reported for C8-BTBT layer prepared on quartz substrate.[17] The optical band gap energy was evaluated from the absorption edge wavelength by using following equation,

$$Eb = h\nu = hc/\lambda_{ae}, \quad (1)$$

where, $Eb$, $\lambda_{ae}$, $h$, $c$, and $\nu$ are band gap energy, absorption edge wavelength, Planck constant, velocity of light, and frequency.[18] The bandgap energy was estimated by extrapolating the linear part to $\alpha = 0$ on the relationship between the photon energy and absorption coefficient was calculated from the absorbance and thickness. The optical band gap energy of C8-BTBT layers was estimated to be 3.32–3.35 eV regardless of the layer thickness and preparation temperature. The absorption coefficient at 358 nm wavelength was calculated from the absorbance and thickness and ranged from $3.2 \times 10^4$ to $6.8 \times 10^4\,cm^{-1}$.

**Figure 7** shows the resistivity of C8-BTBT layers prepared at 300, 343, and 373 K without light irradiation and with AM1.5G light irradiation. The resistivity was estimated by van-der-Pauw technique with Hall-effect measuring system with and without light irradiation, but the carrier concentration and mobility could not be estimated in this technique. The resistivity in dark drastically decreased from $2.1 \times 10^6$ to $1.2 \times 10^2\,\Omega\,cm$ with increase in preparation temperature from 300 to 373 K. The (002) peak angle and preferred orientation were almost the same for all C8-BTBT layers. The grain size, however, changed

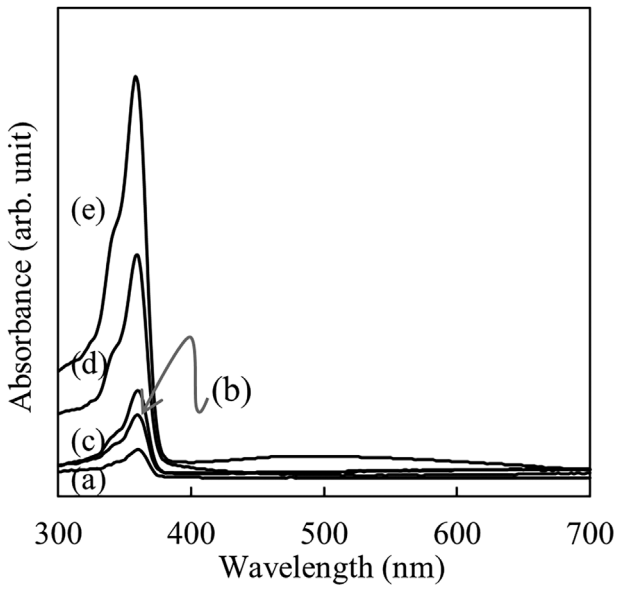


**Figure 6.** Optical absorption spectra of 5 (a), 10 (b), 15 (c), 50 (d), 100-nm-thick-C8-BTBT layers (e) prepared on C-sapphire substrate at 300 K.

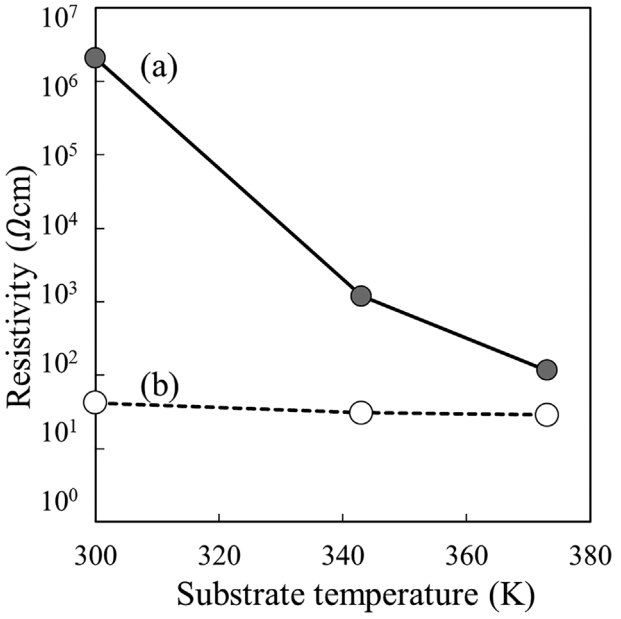


**Figure 7.** Resistivity of 100-nm-thick-C8-BTBT layers prepared at 300–373 K without light irradiation (a), and with AM 1.5G light irradiation (b).

depending on the preparation temperature. The grain boundary act as scattering defects for transporting carrier as reported in inorganic semiconductors,[19,20] although the carrier transporting phenomena is deflect among organic and inorganic semiconductor. The result revealed that the grain size was an important factor affecting to the resistivity of C8-BTBT layers in dark.

The resistivity drastically decreased to 42–28 Ω cm by irradiating the light. As the AM1.5G light irradiated to C8-BTBT layers contained a light at the photon energy higher than the bandgap energy, the excitation of electron was occurred inside the C8-BTBT molecules. Although further investigation is needed on the electrical characteristics, the light irradiation affects the carrier transporting phenomenon inside the grains.

## 4. Conclusions

C8-BTBT layers were prepared on a single crystal (0001) $Al_2O_3$ (C-sapphire) substrate by a vacuum evaporation technique, and the (001) out-of-plane orientation were developed irrespective of the prepration condition of the thickness and preparation temperature. The C8-BTBT layer was formed by the growth of (001)-C8-BTBT islands in direction parallel to the substrate surface and then the growth in direction normal to the substrate surface after the formation of the continuous layer. The optical band gap energy was estimated to be 3.32–3.35 eV. The resistivity of 100 nm thick C8-BTBT layers in dark decreased from $2.1\times10^{6}$ to $1.2\times 10^{2}$ Ω cm with increasing the preparation temperature 300–373 K, and the resistivity value also decreased to 42–28 Ω cm by a light irradiation.

## Acknowledgements

The authors are grateful to the finanicial support (Kakenhi, 16K12649) of Japan Society for the Promotion of Science (JSPS).

## Conflict of Interest

The authors declare no conflict of interest.

## Keywords

C8-BTBT, growth behavior, organic electronics, vacuum thermal evaporation

Received: November 9, 2017
Revised: January 29, 2018
Published online: March 5, 2018

[1] X. Guo, M. Baumgarten, K. Müllen, *Prog. Polym. Sci.* **2013**, *38*, 1832.
[2] A. Facchetti, *Mater. Today.* **2007**, *10*, 28.
[3] L. Bian, E. Zhu, J. Tang, W. Tang, F. Zhang, *Prog. Polym. Sci.* **2012**, *37*, 1292.
[4] Y. Guo, G. Yu, Y. Liu, *Adv. Mater.* **2010**, *22*, 4427.
[5] F. Dinelli, M. Murgia, P. Levy, M. Cavallini, F. Biscarini, *Phys. Rev. Lett.* **2004**, *92*, 116802.
[6] N. Karl, *Synth. Met.* **2003**, *134*, 649.
[7] S. Wang, D. Niu, L. Lyu, Y. Huang, X. Wei, C. Wang, H. Xie, Y. Gao, *Appl. Surf. Sci.* **2017**, *416*, 696.
[8] G. Gbabode, M. Dohr, C. Niebel, J. Y. Balandier, C. Ruzié, P. Négrier, D. Mondieig, Y. H. Geerts, R. Resel, M. Sferrazza, *ACS Appl. Mater. Interfaces.* **2014**, *6*, 13413.
[9] Y. Yuan, G. Giri, A. L. Ayzner, A. P. Zoombelt, S. C. B. Mannsfeld, J. Chen, D. Nordlund, M. F. Toney, J. Huang, Z. Bao, *Nat. Commun.* **2014**, *5*, 1.
[10] T. Uemura, Y. Hirose, M. Uno, K. Takimiya, J. Takeya, *Appl. Phys. Express.* **2009**, *2*, 111501.
[11] H. Minemawari, T. Yamada, H. Matsui, J. Tsutsumi, S. Haas, R. Chiba, R. Kumai, T. Hasegawa, *Nature* **364**, *475*.
[12] C. Liu, T. Minari, X. Lu, A. Kumatani, K. Takimiya, K. Tsukagoshi, *Adv. Mater.* **2011**, *23*, 523.
[13] L. Lyu, D. Niu, H. Xie, N. Cao, H. Zhang, Y. Zhang, P. Liu, Y. Gao, *J. Chem. Phys.* **2016**, *144*, 034701.
[14] D. He, Y. Zhang, Q. Wu, R. Xu, H. Nan, J. Liu, J. Yao, Z. Wang, S. Yuan, Y. Li, Y. Shi, J. Wang, Z. Ni, L. He, F. Miao, F. Song, H. Xu, K. Watanabe, T. Taniguchi, J.-B. Xu, X. Wang, *Nat. Commun.* **2014**, *5*, 5162.
[15] T. Izawa, E. Miyazaki, K. Takimiya, *Adv. Mater.* **2008**, *20*, 3388.
[16] Joint Committee on Powder Diffraction Standards, Powder Diffraction File (International Data for Diffraction Data) pp 042-1468.
[17] R. Miscioscia, F. Loffredo, G. Nenna, F. Villani, C. Minarini, M. Petrosino, A. Rubino, M. Denti, A. Facchetti, *Physics, Mater. Appl.* **2016**, *30*, 83.
[18] J. C. S. Costa, R. J. S. Taveira, C. F. R. A. C. Lima, A. Mendes, L. M. N. B. F. Santos, *Opt. Mater. (Amst).* **2016**, *58*, 51.
[19] T. Shinagawa, M. Onoda, B. M. Fariza, J. Sasano, M. Izaki, *J. Mater. Chem. A.* **2013**, *1A*, 9182.
[20] T. Shinagawa, M. Chigane, K. Murase, M. Izaki, *J. Phys. Chem. C* **2012**, *116C*, 15925.